

A Seminar Report on

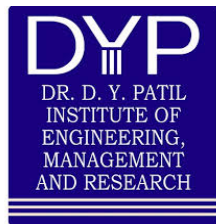
Study of Aerospike Engine and Performance Comparison With Conventional Bell-Cone Type Nozzle

By

Mr. Bhoge Yugesh

Guided by

Mr. Vishal Solapure



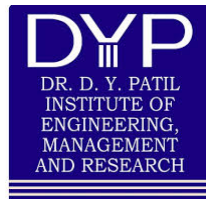
Department of Mechanical Engineering

**Dr. D. Y. Patil Institute Of Engineering,
Management & Research**

Akurdi

[2018-19]

**Dr. D. Y. Patil Institute Of Engineering,
Management & Research
Akurdi**



C E R T I F I C A T E

This is to certify that Mr. Bhoge Yugesh, has successfully completed the Seminar work entitled "Study of Aerospike Engine and Performance Comparison With Conventional Bell-Cone Type Nozzle" under my supervision, in the partial fulfilment of Bachelor of Engineering - Mechanical Engineering, by Savitribai Phule Pune university

Date :

Place :

Mr.Vishal Solapure
(Guide)

Prof. Kiran .N. Narkar
(Head of Department)

External Examiner
Dr. A.V. Patil
(Principal)

Acknowledgement

It gives me great pleasure in presenting the seminar report on ‘Study of Aerospike Engine and Performance Comparison With Conventional Bell-Cone Type Nozzle’. I would like to take this opportunity to thank my internal guide Prof. V. Solapure for giving me all the help and guidance I needed. I am really grateful to him for his kind support. His valuable suggestions were very helpful. I am also grateful to Prof. K.M Narkar, Head of Mechanical Engineering Department, DYPIEMR for his indispensable support, suggestions.

Yugesh Bhoge

T.E Mech Engg

Abstract

Single-stage to orbit (SSTO) rocket technology offers the potential to substantially reduce launch costs, but has yet to be considered practical for conventional launch vehicles. However, new research in composite propellant tank technology opens the field for renewed evaluation. One technology that increases the efficiency and feasibility of SSTO flight is an altitude compensating rocket engine nozzle, as opposed to a conventional constant area, bell nozzle design. By implementing an altitude compensation nozzle, such as a linear, aerospike nozzle for in-atmosphere flight, the propellant mass fraction (PMF) may be reduced by as much as seven percent compared to a conventional rocket engine. Results suggest that having a limited nozzle configuration, where the nozzle is not allowed to expand to infinity, further increases the engine efficiency by lowering the PMF by 0.1-0.2 %. Additional modeling is required to confirm this, but it is evident that altitude compensating nozzles perform better than the conventional bell nozzles used in these simulations.

Keywords:- SSTO, PMF, aerospike, efficiency, altitude compensating nozzles.

Index

Sr .No	Content	Page no
1.1	Introduction	1
1.1.1	Introduction to Aerospike Nozzle:	1
1.1.2	Design and Purpose	
1.1.3	Comparison to Bell and Cone Nozzle Designs	2
1.2	Literature review	
1.2.1	Current work	7
1.3	Mathematical model	8
1.3.1	Nozzle Theory	8
1.3.2	Launch vehicle mechanics	10
1.3.3	Basic equation	10
1.4	Experimental Setup	13
1.5	Results	14
1.6	Conclusion	17
1.7	References	18

List of figures

Content	Page No
Figure 1: Aerospike Nozzle, Exhaust Plume Diagram at High (overexpanded), Optimized (perfectly expanded), and Low (underexpanded) Ambient Pressures	2
Figure 2: Bell Nozzle, Exhaust Plume Diagram at High (overexpanded), Optimized (perfectly expanded), and Low (underexpanded) Ambient Pressures.	2
Figure 3: Conical Nozzle, Exhaust Plume Diagram at High (overexpanded), Optimized (perfectly expanded), and Low (underexpanded) Ambient Pressures.	3
Figure 4: Hyperion Configuration	4
Figure 5: Lockheed Martin Linear Aerospike Hot Fire Test as Part of the LASRE Program	6
Figure 6: California State University Curved vs. Linear Aerospike Thruster Design	6
Figure 7: Rocket Engine Basic Design	8
Figure 8: Cross-section of Conical Plug Spike Nozzle, Exhaust Plume Diagram at High (overexpanded), Optimized (perfectly expanded),	10
Figure 9: Launch Vehicle Trajectory Diagram	11
Figure 10: CFD Analysis	13

List of table

Content	Page No
Table No.01: Boundary Condition for CFD in Vacuum	13
Table No.02: Boundary Condition for CFD at Sea Level	13
Table No.03: Results of CFD in Vacuum	14
Table No.04: Results of CFD at Sea Level	14
Table No.05: Values of Cf at different altitude	14
Table No.06: Values of PMF at different altitude	15

List of Graphs

Content	Page No
Graph 01: Altitude V/s Thrust coefficient (Cf)	15
Graph 02: Altitude V/s PMF	16

1.1 INTRODUCTION:

1.1.1 Introduction to Aerospike Nozzle:

Reducing the cost of space travel is an ongoing launch optimization problem. One accepted method to accomplish this is through single-stage to orbit (SSTO) flight, which reduces the launch weight by simplifying the design. Previous work has evaluated the feasibility of SSTO through new composite propellant tank technology [1] in an effort to reduce the dry mass of the system; with the addition of an updated nozzle design, the propellant mass fraction (PMF, defined in Section 1.3.3) may be reduced even further, leaving more weight available for payload. The dry mass refers to the mass of the system without the propellant; this includes the structure, engine, instrumentation, payload, etc. The wet mass is the total mass of the system, including the propellant.

1.1.2 Design and Purpose:

The annular, aerodynamic spike nozzle, also known as an aerospike, is a variable exit area nozzle designed to maintain perfect expansion throughout flight by compensating for the change in ambient pressure as a result of the increasing altitude. The aerospike nozzle is shown in Figure 1 (black trapezoid) with its corresponding exhaust plume conditions. The aerospike design is essentially an inverted nozzle where, instead of the exhaust flow being contained inside a structure, the flow is directed around a structure with the ambient pressure acting as the outer boundary. At low altitudes, when the ambient pressure is highest, the exhaust remains close to the nozzle contour, maintaining isentropic expansion (far left image). The aerospike nozzle is at maximum efficiency when the exhaust gases form a column, parallel to the direction of flight. The middle image of Figure 1 shows the exhaust plume in this parallel direction a short distance downstream. At higher altitudes, recompression shock waves occur inside the plume, forcing the plume to remain column-shaped in a closed-wake state [4] (far right image), despite the expanding exhaust plume shape. This maintains efficiency because the exhaust gases are not expanding beyond the physical nozzle, but still exerting force, thus producing thrust, on the nozzle itself. The advantages of the aerospike design compared to a constant area nozzle are that it maintains higher efficiency for a greater flight path and that the primary flow is acted upon only by the ambient pressure of the atmosphere. Some disadvantages of the aerospike design include its

increased mass, thermal cooling considerations, and increased cost to manufacture due to the complexity of the design. Other configurations of the annular nozzle design are discussed.

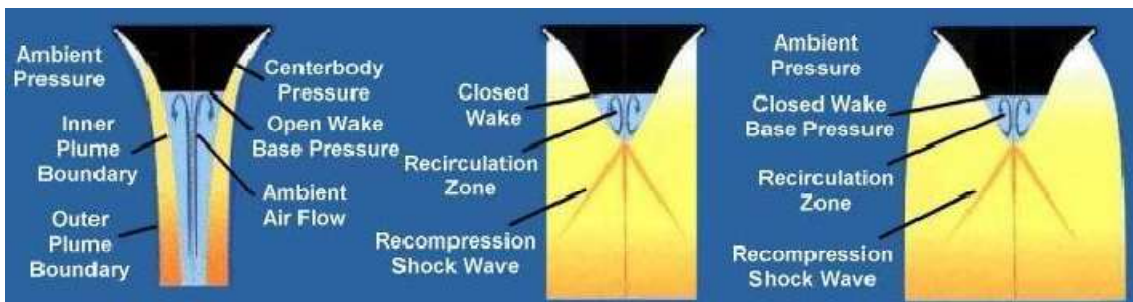


Figure 1: Aerospike Nozzle, Exhaust Plume Diagram at High (overexpanded), Optimized (perfectly expanded), and Low (underexpanded) Ambient Pressures [1].

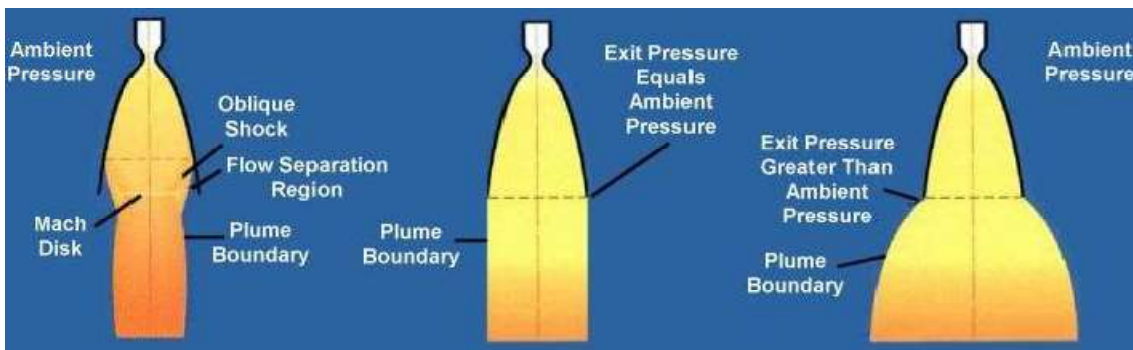


Figure 2: Bell Nozzle, Exhaust Plume Diagram at High (overexpanded), Optimized (perfectly expanded), and Low (underexpanded) Ambient Pressures [1].

1.1.3 Comparison to Bell and Cone Nozzle Designs:

Most rockets today have the traditional bell nozzle design on their engines as shown in Figure 2. It is the most efficient, conventional nozzle design currently in use. At lower altitudes, where the ambient pressure is high, the exhaust gases are overexpanded inside the nozzle and compressed radially inwards towards the nozzle exit. In extreme cases this can cause flow separation from the boundary wall within the nozzle, decreasing efficiency. When the exit pressure of the exhaust gases equals that of the ambient, the engine is at maximum efficiency because the thermal energy of the plume that is being converted directly into directed kinetic energy to produce thrust is maximized. As the rocket continues to increase in altitude, the ambient pressure continues to decrease. The exhaust gases are under expanded at the nozzle exit, when the ambient pressure is less than the pressure at the nozzle exit, causing the exhaust to continue to expand beyond the nozzle. This

external expansion does not exert force on the nozzle wall, so that is thrust lost, decreasing the engine efficiency. This under expansion is a lost opportunity and would not be a loss by having a larger nozzle exit area to achieve higher nozzle exit velocities, as the aerospike configuration allows. These exhaust plume behaviors describe basic compressible gas expansion, when a gas at high pressure and density is expanded isentropically to larger volumes in order to reduce its pressure and density. In Figure 2, the exhaust gases expanding in a fixed-area nozzle experience overexpansion, then perfect expansion, then underexpansion as altitude is increased. This suggests that a variable nozzle exit area should optimize engine performance if all other parameters are held equal.

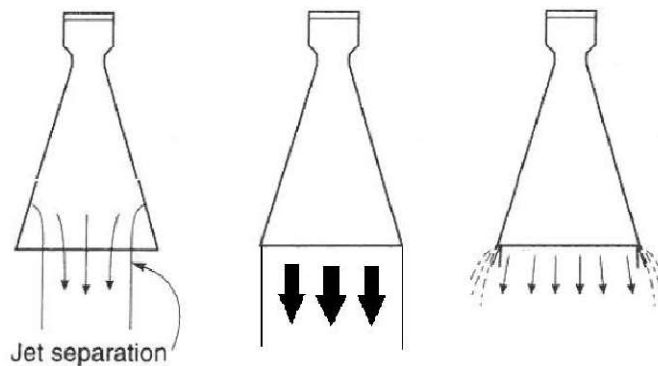


Figure 3: Conical Nozzle, Exhaust Plume Diagram at High (overexpanded), Optimized (perfectly expanded), and Low (underexpanded) Ambient Pressures [7].

1.2 LITERATURE REVIEW:

1.2.1.1 Single-Stage to Orbit Flight:

When the United States first decided to dedicate a focused effort towards space flight in the late 1950s, the idea of SSTO was already under consideration as a possible method to achieve orbit. At the time however, it was deemed infeasible due to material and technological limitations of the time. SSTO technology remained on the back burner until the Challenger disaster in 1986. As a result of this event, all rocket technology was reevaluated, and for the next decade, a serious effort was made into the analysis and feasibility of SSTO

[7]. The primary focus of SSTO development in the mid-1990s focused on multiplepropellant engines, proposing that either dual mixture engines (oxygen and hydrogen propellants) [3], or that tri-propellant engines would increase performance of new engines [2] or existing engines [8]. Many private corporations were hesitant to commence development of this technology until the conclusion of the joint NASA/Lockheed Martin X-33 project [3] (see Section 1.2.1.3). Finally, Dorrington of the University of London said at the turn of the century that only expendable SSTO technology was possible and that cheaper engines with greater reliability would need to be developed in order to truly make SSTO feasible [8]. The author feels that the ongoing advances in materials technology increases the feasibility of SSTO technology.

1.2.1.2 Georgia Tech Hyperion:

One example of the evaluation of SSTO was a Georgia Institute of Technology project sponsored by NASA Marshall Space Flight Center entitled Hyperion [3]. The primary purpose of this project was to determine if a rocket-based combined cycle (RBCC) could be used to produce a vehicle that could reduce the cost of space flight. Georgia Tech proposed a plan for a horizontal takeoff and horizontal landing (HTHL) vehicle for SSTO that uses five ejector 7 scramjet RBCC engines, combusting LOX/LH₂. Their concept is presented in Figure 4. The basic design for Hyperion incorporated both advanced propulsion techniques as well as metal composites.

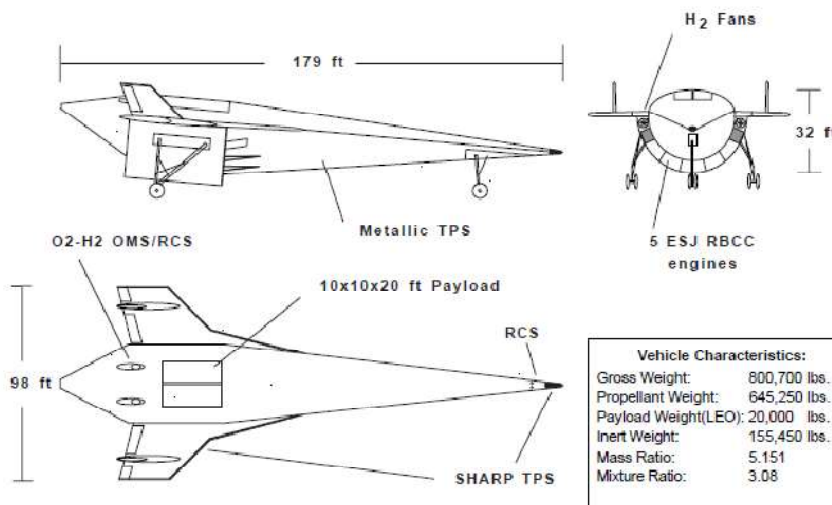


Figure 4: Hyperion Configuration [2]

Georgia Tech used the Simulated Combined Cycle Rocket Engine Analysis Module (SCCREAM), a one-dimensional analysis code outputting an engine deck for use in a trajectory simulation program. The trajectory analysis was performed in the Program to Optimize Simulated Trajectories (POST) [2], a NASA/Lockheed Martin counterpart to OTIS. The trajectory constraint was a dynamic pressure boundary of 2,000 psf during the ramjet and scramjet modes, when the Hyperion flies between Mach 3 and 9, as any higher pressure loading would increase airframe weight and cooling requirements. Transition to the all-rocket mode is completed by Mach 10. This vehicle was designed to be low cost and reusable at about 150 flights a year at \$1.64M a flight in 1999. Georgia Tech determined that the probability of achieving a viable Hyperion was low as it did not present a reduction in cost of existing vehicles, thus a prototype was never constructed.

1.2.1.3 NASA/Lockheed Martin Linear Aerospike SR-71 Experiment:

In 1997, Rocketdyne, now a division of Boeing, published their results for the Linear Aerospike SR-71 Experiment (LASRE) program to demonstrate the performance of the linear 12 aerospike on a lifting body to specifically simulate the X-33 [4]. This was accomplished by mounting a 20% scale, X-33 forebody onto an SR-71 (Lockheed Martin Blackbird) to determine the magnitude of the slipstream effect at the proper altitude and Mach number conditions before starting hot fire tests of the engine. The slipstream effect refers to the degradation of engine performance due to the air moving over the lifting body interacting with the outer boundary of the exhaust plume. The data from this test was used to validate computational fluid dynamic (CFD) codes for future vehicle design and optimization. The X-33 was the subscale technology demonstrator for a NASA-Lockheed Martin joint project known as the Venture Star. The Venture Star was a proposed, SSTO reusable launch system that was never fully developed due to complications with the weight associated with the LASRE and X-33 programs [9]. The major study on the LASRE project and its application for the Venture Star was a trajectory optimization study in how to generate a parametric model for optimizing aerospike designs [1]. NASA Langley Research Center was able to successfully generate an aerospike engine database by using POST and integrated the resulting parametric model into a multidisciplinary framework in order to determine alternate designs. In 2001, Lockheed Martin was able to perform a hot fire test, shown in Figure 5.

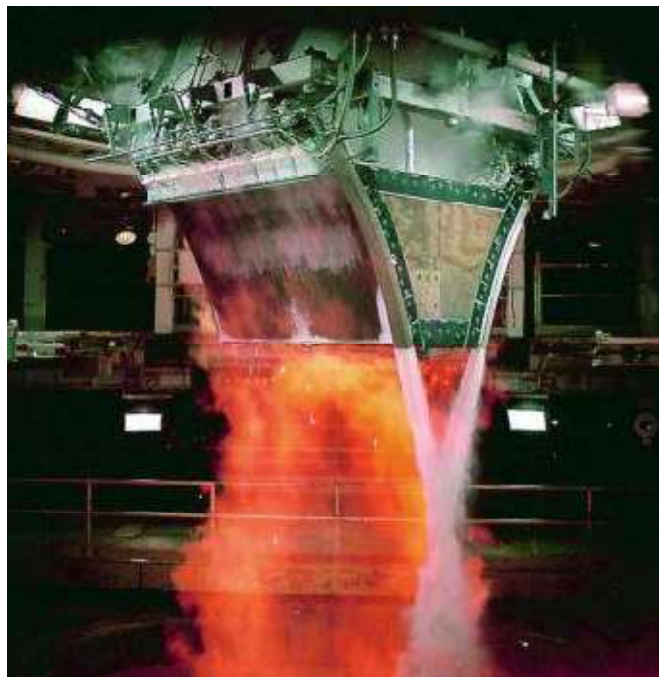


Figure 5: Lockheed Martin Linear Aerospike Hot Fire Test as Part of the LASRE Program [5].

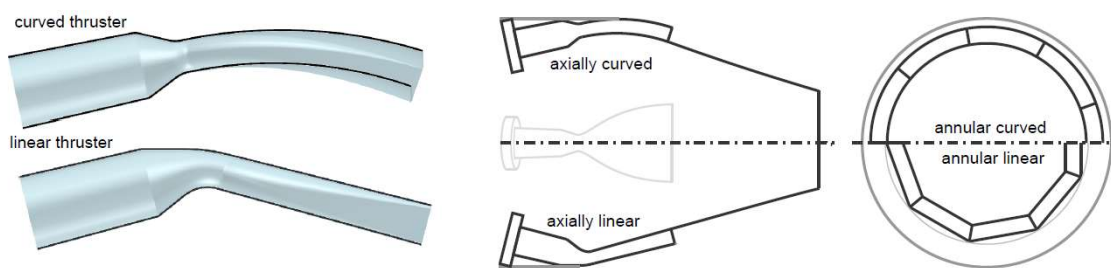


Figure 6: California State University Curved vs. Linear Aerospike Thruster Design [5].

1.2.1 Current Work:

Since the lack of progress associated with the LASRE and X-33 projects in 2001, there has been little funding dedicated to the continued development of the linear aerospike engine. Furthermore, a lack of advancement in materials science has impeded the progress into SSTO technology.

1.2.1.1 SKYLON Spaceplane :

Reaction Engines, Ltd., a British corporation founded in 1989, has developed the concept of a SKYLON spaceplane to act as a horizontal takeoff, horizontal landing, SSTO vehicle that uses two of their in-house developed SABRE engines [4]. SABRE is an air-breathing rocket based combined cycle (RBCC) engine. It uses the oxygen in the air at low altitudes combined with liquid hydrogen fuel for combustion, then switches to a conventional rocket mode at high altitudes using on-board liquid oxygen as the oxidizer. This reduces the weight of the vehicle allowing for greater payloads. With the SABRE engines, SKYLON is designed to carry up to 9.5 tons of payload to a 460 kilometer altitude. This technology has yet to be fully tested or integrated at the time of this seminar.

1.2.1.2 Firefly :

A relatively new company, Firefly, has just emerged proposing a satellite launch design entitled Firefly Alpha [1]. This 2-stage, carbon composite structure is designed to launch a 400 kg payload to low Earth orbit (LEO). The first propulsion stage uses a plug-cluster aerospike design² with a liquid oxygen and methane propellant. There have been no published details on their design, but what details they do have is provided on the company website.

1.3 MATHEMATIC MODEL:-

1.3.1 Nozzle Theory:

There are a few characteristic parameters to describe the dynamics of compressible fluid flow as applied to a rocket engine nozzle. The first, the Mach number, M, describes the relationship of the local speed, V, to the local speed of sound, a, as shown in Equation 1. A Mach number less than one describes the subsonic flow regime, equal to one is the sonic condition, and between one and approximately five is supersonic. A Mach number greater than about five is considered hypersonic, with non-negligible thermodynamic considerations associated with noncalorically perfect gases such as a chemically reacting flow.

$$M = V/a \quad (1)$$

The basic configuration for a rocket engine nozzle is shown in Figure 13. For the cases evaluated in this seminar, the fuel was liquid hydrogen (LH₂), and the oxidizer was liquid oxygen (LOX). It was assumed that the conditions in the combustion chamber remained constant, such that the resulting exhaust gas was ideal and calorically perfect under a constant pressure. This requires the assumption of non-reacting flow during nozzle expansion. This is commonly called “frozen flow”. The other extreme is called “equilibrium flow”, where reactions occur at a rate so high that conditions continuously adjust in order to maintain equilibrium at the local pressure and enthalpy levels; this makes the entire process reversible [2].

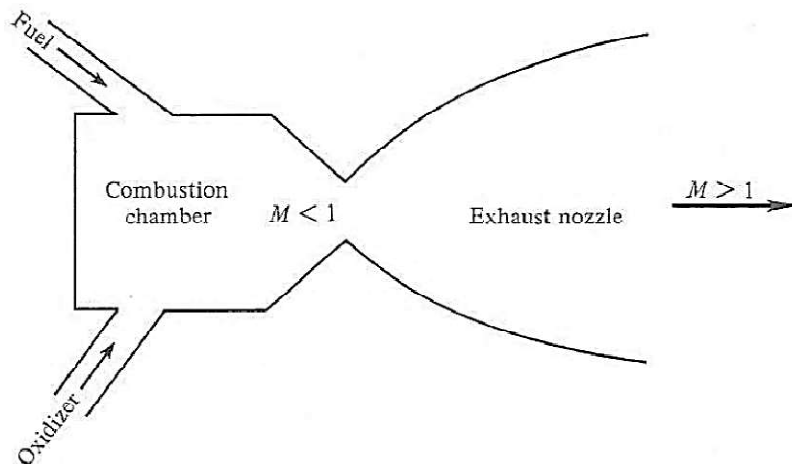


Figure 7: Rocket Engine Basic Design [2].

The thermally ideal gas relation, provided in Equation 2, was also assumed to be applicable with P, the pressure, v, the mass specific volume, ρ, the density, R, the universal gas constant, and T, the absolute temperature.

$$Pv = \rho RT \quad (2)$$

There are several characteristic equations that define the relationship of particular parameters between the throat, nozzle exit, and combustion chamber locations. These are summarized below in Equations 3 – 5 for a thermally and calorically perfect gas. The superscript, *, indicates sonic conditions at the throat, while the subscript, 0, represents the chamber (stagnation) conditions, with γ being the specific heat ratio:

$$P* = P_0[(\gamma + 1)/2]^{-\gamma/(\gamma-1)} \quad (3)$$

$$T* = T_0[2(\gamma + 1)] \quad (4)$$

$$a* = \sqrt{\gamma RT*} \quad (5)$$

The isentropic pressure ratio, Equation 6, between the chamber and the nozzle exit is written in terms of the Mach number, M, as well as the area-Mach relation equation, Equation 7, which relates the nozzle exit, A_e , and throat, A^* , areas.

$$P_0/P = [1 + ((\gamma - 1)/2)M^2]^{\gamma/(\gamma-1)} \quad (6)$$

$$A_e/A^* = (1/M^2)[(2/(\gamma + 1))(1 + ((\gamma - 1)/2)M^2)]^{(\gamma+1)/(\gamma-1)} \quad (7)$$

These equations relate nozzle local (exit) pressure and area to chamber (stagnation) values for perfect expansion flow of an optimal nozzle profile, forming the basis for nozzle theory and analysis.

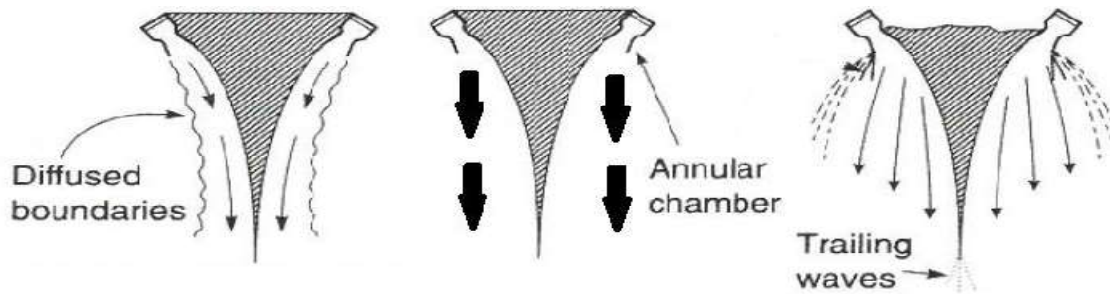


Figure 8: Cross-section of Conical Plug Spike Nozzle, Exhaust Plume Diagram at High (overexpanded), Optimized (perfectly expanded), and Low (underexpanded) Ambient Pressures [3].

1.3.2 Launch Vehicle Mechanics:

The purpose of a rocket engine is to use the chemical energy from combusting propellant, LOX/LH₂ for the purpose of this seminar, to produce a large quantity of high pressure gas, which is expanded and accelerated through a nozzle to provide thrust. This principle is based on Newton's balance of momentum which states that when mass is ejected from a system (the propellant) in one direction, the mass left behind acquires a velocity in the opposite direction (the rocket and payload). This section introduces the fundamental equations that describe rocket trajectories and performance.

1.3.3 Basic Equations:

The basis for describing the trajectory of a rocket is presented in Figure 9. The engines at the base of the rocket produce the thrust, T, acting in the direction of the velocity vector, v. In the figure, the velocity is broken into a tangential and normal unit vectors; the tangential vector is in the same direction as the velocity, while the normal vector is perpendicular to the velocity direction and points towards the center of curvature, C. The drag force, D, is an aerodynamic force acting opposite to the velocity. The drag forces depend on the dynamic pressure, the drag coefficient, and a reference surface area. The angle, α , in Figure 9, is the flight path angle, described in relation to the trajectory model. The dynamic pressure, q, defines the kinetic energy per unit volume of the fluid as a function of the density, ρ , and the local speed, V, shown in Equation 8.

$$q = \frac{1}{2} \rho V^2 \quad (8)$$

The overall thrust, T , is defined in Equation 9 with ue , the nozzle exit velocity, Ae , the nozzle exit area, and Pe , the nozzle exit pressure. The mass flow rate, \dot{m} , is the rate of the combusted gases moving through the nozzle. The static pressure, P , is the local ambient pressure at altitude.

$$T = \dot{m} ue + Ae (Pe - P) \quad (9)$$

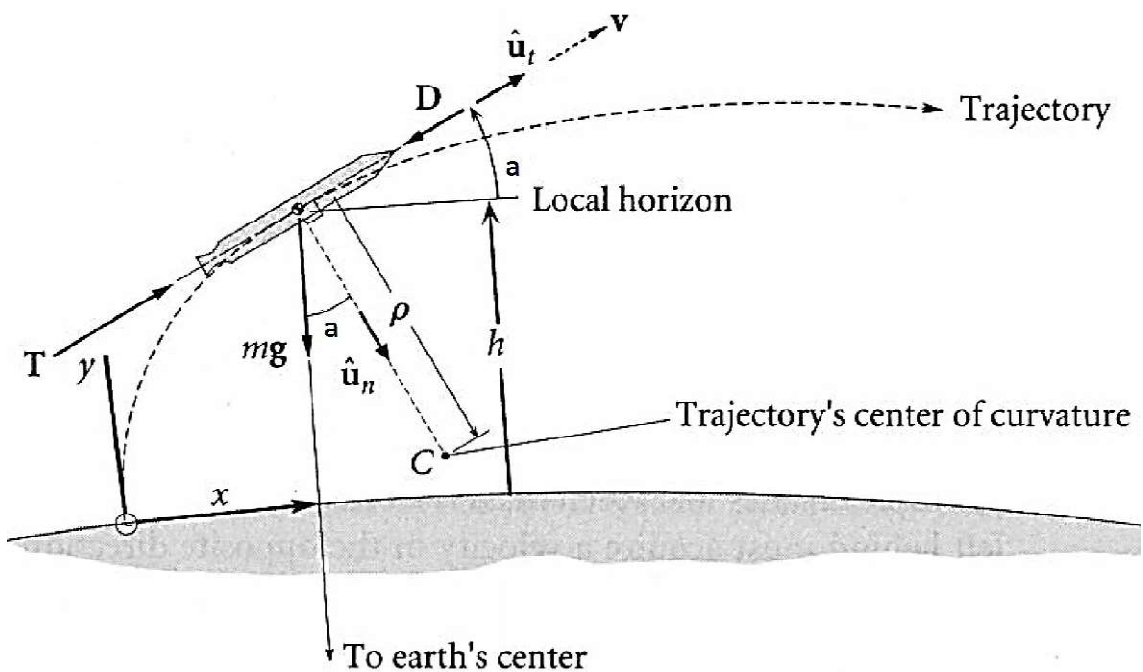


Figure 9: Launch Vehicle Trajectory Diagram [7]

The final performance parameter, which serves as the basis for trajectory comparison and optimization in this seminar, is the propellant mass fraction (PMF). The PMF represents what percentage of the total mass (weight) that is propellant consumed during flight [13]; this was calculated for each trajectory by using Equation 10.

$$PMF (\%) = [(W_i - W_f)/W_i] \times 100 \quad (10)$$

In this equation, it is assumed that all propellant is consumed during flight so that the difference between the initial weight, W_i , and the final weight, W_f , is the propellant weight.

Thus, as the PMF decreases, less propellant is consumed to reach the same altitude, allowing for delivery of greater payloads.

1.4 EXPERIMENTAL SETUP:

Boundary conditions for computational fluid dynamics (CFD) analysis are;

1) At Vacuum:-

Flow Pressure Gauge total pressure Inlet	3E+05 Pa
Flow Pressure Gauge static pressure Outlet	0 Pa
Flow Option at wall	No slip
Material	Air Ideal Gas

Table No.01: Boundary Condition for CFD in Vacuum

2) At Sea level:-

Flow Pressure Gauge total pressure Inlet	3E+05 Pa
Flow Pressure Gauge static pressure Outlet	0 Pa
Flow Option at wall	No slip
Material	Air Ideal Gas

Table No.02: Boundary Condition for CFD at Sea Level

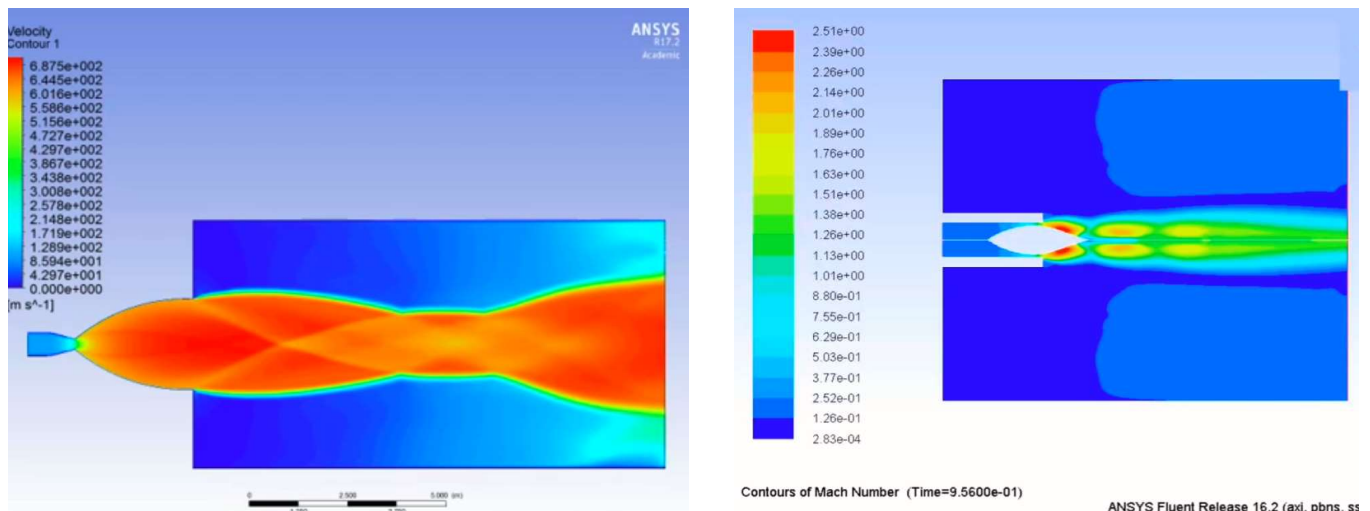


Figure 10: CFD Analysis upon conventional BELL-CONE type nozzle (on left) and AEROSPIKE nozzle(on right).

1.5 RESULTS:

1) At Vacuum:

Result	Variable	Location	Calculated minimum	Calculated maximum	Calculated average
Temperature 1	Temperature	Inlet 1	2200.7 [C]	2500 [C]	2491.6 [C]
Temperature 2	Temperature	Outlet 1	1246.9 [C]	2502.9 [C]	1739.3 [C]
Vector	Variable	Location	Calculated minimum	Calculated maximum	Calculated average
Velocity 1	Velocity	1 volume	0 [m s^-1]	1435 [m s^-1]	925.74 [m s^-1]

Table No.03: Results of CFD in Vacuum

2) At Sea Level:

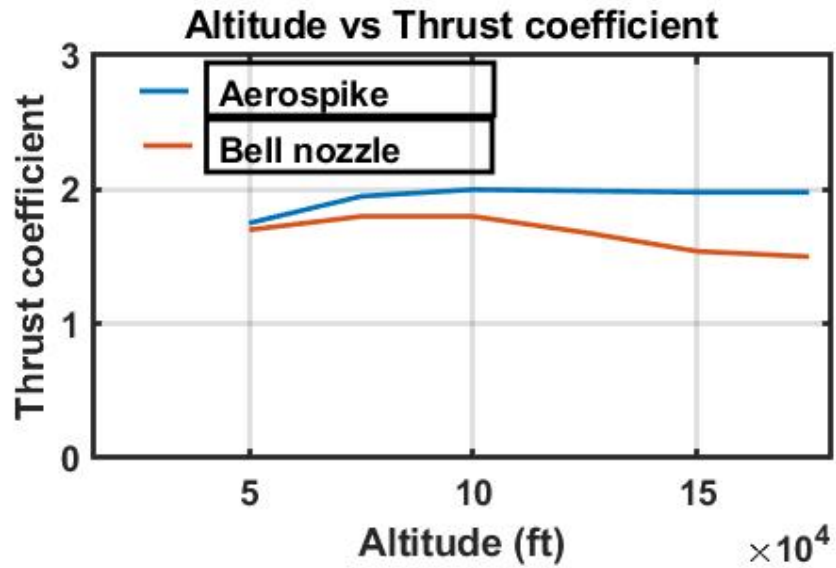
Result	Variable	Location	Calculated minimum	Calculated maximum	Calculated average
Temperature 1	Temperature	Inlet 1	2200.7 [C]	2500 [C]	2491.6 [C]
Temperature 2	Temperature	Outlet 1	1246.9 [C]	2502.9 [C]	1739.3 [C]
Vector	Variable	Location	Calculated minimum	Calculated maximum	Calculated average
Velocity 1	Velocity	1 volume	0 [m s^-1]	1588.2 [m s^-1]	833.15 [m s^-1]

Table No.04: Results of CFD at Sea Level

3) Altitude vs Thrust coefficient:

Altitude(ft)	Aerospike Nozzle	Bell Nozzle
50000	1.75	1.7
75000	1.95	1.8
100000	2	1.8
125000	1.99	1.68
150000	1.98	1.54

Table No.05: Values of C_f at different altitude

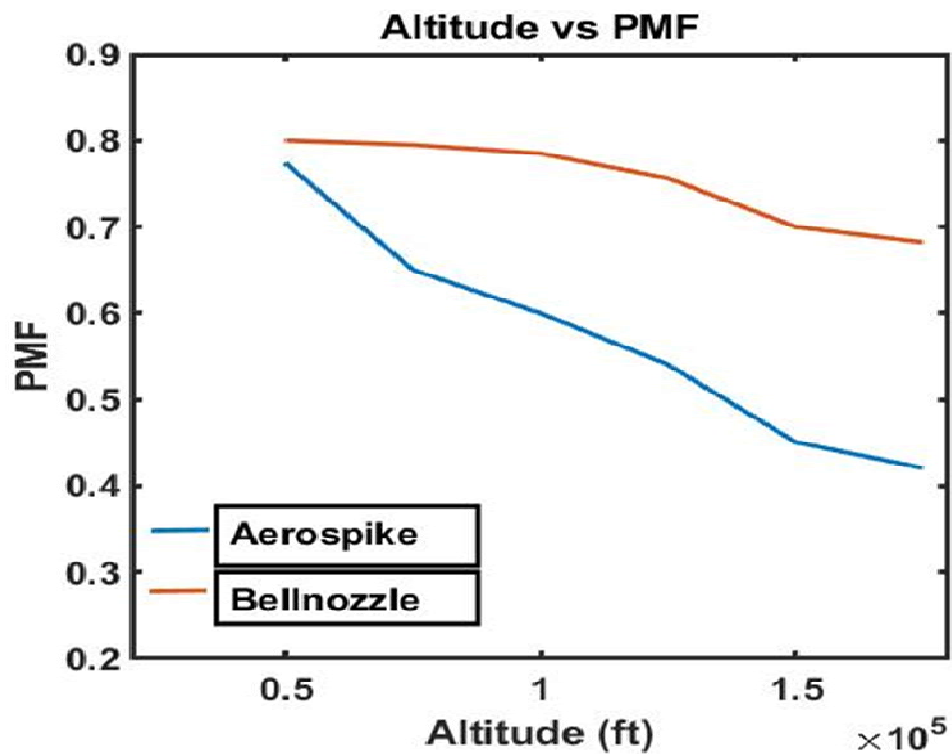


Graph 01: Altitude V/s Thrust coefficient (C_f)

4) Altitude vs PMF:-

Altitude(ft)	Aerospike Nozzle	Bell Nozzle
50000	0.774	0.8
75000	0.6502	0.7948
100000	0.6	0.785
125000	0.5405	0.7562
150000	0.4507	0.7

Table No.06: Values of PMF at different altitude



Graph 02: Altitude V/s PMF

From the graphs it has clearly been seen that as the altitude increases thrust coefficient of aerospike nozzle first increases and then remains constant and for conventional bell nozzle it is first slowly increases and then decreases. And the thrust coefficient of aerospike at all the altitudes is greater than the that of conventional bell nozzle. And the pmf of aerospike is rapidly decreases as compared to that of that of conventional bell cone type nozzle.

1.5 CONCLUSION:

With new technology that focuses on the feasibility of SSTO being developed, the evaluation of rocket nozzles may further optimize this method of space travel. The use of an annular, aerodynamic spike nozzle, instead of the traditional bell design, optimizes an unmanned, heavy launch vehicle by lowering the propellant mass fraction (PMF) up to 7% from conventional rocket engine designs.

Aerospike engines inherently have a higher specific impulse value than bell nozzle designs, and the results show that this can have a significant impact on performance.

1.7 REFERENCES

- [1] Charles E. Hall, Hagop V. Panossian, “X-33 Attitude Control Using The Xrs-2200 ‘Linear Aerospike Engine’”. June2004
- [2] J. J. Korte,“Parametric Model Of An Aerospike Rocket Engine”, Aiaa 2000-1044, Jan 2000
- .
- [3] Mohammed Imran, “Introduction To Aerospike And Its Aerodynamic Features”, Issn 2250-3153. May 2016.
- [4] Hagop Panossian, Richard Nelson, Hoi Tran, Jeff Klop, Robert Aguilar ,Chuong Luu,“Aerospike Engine Control System Features And Performance”, 6633, July2000.
- [5] Lockheed Martin, [Online] (<https://www.lockheedmartin.com/en-us/index.html>)
[09/04/2019].
- [6] Nasa’s Marshall Space Flight Centre, [Online],
(<https://www.nasa.gov/centers/marshall/news/background/facts/aerospike.html>).
[09/04/2019].
- [7] Nasa Hq, [Online],(https://www.hq.nasa.gov/pao/history/x-33/aero_faq.htm)
[07/03/2019].
- [8] Arca Haas2ca, [Online], (http://www.arcaspace.com/en/haas_2ca/features.htm)
- [9] Wolframalpha, [Online],
(<https://www.wolframalpha.com/input/?i=tsiolkovsky+rocket+equation>)
- [10] A. Chandhra Shekhar, S. Bhargava Satvik Sarma, “CFD Analysis On Conical And Bell Nozzle”, ISSN 2349-4476, June 2017.